Realizations, Characterizations, and Manipulations of Two-Dimensional Electron Systems Floating above Superfluid Helium Surfaces

Haoran Wei(魏浩然)[1,3†], Mengmeng Wu(吴蒙蒙)[2†], Renfei Wang(王任飞)[2], Mingcheng He(何明城)[1,3], Hiroki Ikegami[1], Yang Liu(刘阳)[2*], and Zhi Gang Cheng(程智刚)[1,3,4*]

[1]*Beijing National Laboratory for Condensed Matter Physics, Institute of Physics, Chinese Academy of Sciences, Beijing 100190, China*
[2]*International Center for Quantum Materials, Peking University, Beijing 100871, China*
[3]*School of Physics, University of Chinese Academy of Sciences, Beijing 100049, China*
[4]*Songshan Lake Materials Laboratory, Dongguan 523808, China*

(Received 1 November 2023; accepted manuscript online 23 November 2023)

Electron systems in low dimensions are enriched with many superior properties for both fundamental research and technical developments. Wide tunability of electron density, high mobility of motion, and feasible controllability in microscales are the most prominent advantages that researchers strive for. Nevertheless, it is always difficult to fulfill all in one solid-state system. Two-dimensional electron systems (2DESs) floating above the superfluid helium surfaces are thought to meet these three requirements simultaneously, ensured by the atomic smoothness of surfaces and the electric neutrality of helium. Here we report our recent work in preparing, characterizing, and manipulating 2DESs on superfluid helium. We realized a tunability of electron density over one order of magnitude and tuned their transport properties by varying electron distribution and measurement frequency. The work we engage in is crucial for advancing research in many-body physics and for development of single-electron quantum devices rooted in these electron systems.

DOI: 10.1088/0256-307X/40/12/127301

Confining electrons in two-dimensional spaces underlies a plethora of remarkable electronic and magnetic phenomena. Over the past decades, two-dimensional electron systems (2DESs) have been a focal point of research in condensed matters due to their relevance in both fundamental research and technological applications. Typically realized at interfaces between semiconductors, these systems have yielded ground-breaking insights into topological matters such as integer and fractional quantum Hall effect,[1,2] and unconventional superconductivity.[3–6] Notably, the advent of two-dimensional materials such as graphene[7,8] and transition-metal dichalcogenides (TMDs)[9–11] has reinvigorated the exploration of confined electronic systems. Nevertheless, itinerant electrons in these solid-state systems likely experience interactions with complicated (although periodic in general) potentials exerted by atomic nuclei and valent electrons. The interactions with the local electronic environments limit their mobility. The inevitable presence of disorder and impurities in solid-state systems can also obfuscate the intrinsic electronic behaviors both electrically and magnetically. Unfortunately, these interactions are often unpredictable, thus introducing a formidable barrier for comprehensive understandings on electron behaviors in solid-state systems.

Liquid helium surface offers a unique arena for electron confinements.[12–14] With helium's weak polarizability, a delicate balance can be reached with the attraction between electrons and image charges and the repulsion exerted by helium's potential barrier.[15] It is therefore possible for electrons to be localized by a shallow potential well about 10 nm above the liquid helium surface to form a 2DES.[12,16] Such a 2DES is ideal in many aspects. Firstly, the atomically smooth surface of liquid helium renders an ideal macroscopic substrate that is otherwise extremely difficult to realize on solid surfaces. Secondly, helium's charge neutrality ensures the exemption of electromagnetic interaction with the substrate except the vertical confinement. Thirdly, with the 2DES being completely composed of electrons, the absence of impurities or defects minimizes extrinsic scatterings and guarantees a high mobility. Given with the above-mentioned facts, 2DESs can provide an environment conducive to observing pristine behaviors of electrons as their transport properties are convenient for tuning, enabling a series of phase transitions such as formation of Wigner crystals.[17,18]

Three factors are crucial to realize, characterize, and manipulate 2DESs on helium surfaces: the electron density needs to be easily tuned over a wide range; their motion needs to be properly triggered and detected; and their distribution needs to be precisely controllable. In this Letter, we present comprehensive investigations on such 2DESs from the aspects of preparations, characterizations, and manipulations. The electron density can be controlled within the range of from $3.8\times10^{7}\,\mathrm{cm}^{-2}$ to $3.2\times10^{8}\,\mathrm{cm}^{-2}$;

†These authors contributed equally to this work.
*Corresponding authors. Email: liuyang2@pku.edu.cn; zgcheng@iphy.ac.cn
© 2023 Chinese Physical Society and IOP Publishing Ltd

their motion can be capacitively triggered by voltage modulation and measured in terms of currents; and their distribution can be adjusted by field-effect transistor (FET) technique.

The major components of the experimental setup are enclosed within a copper cell as shown in Figs. 1(a) and 1(b). A printed-circuits board (PCB) is mounted to the cell on which three rectangular copper electrodes with lateral dimensions of $5 \times 10\,\mathrm{mm}^2$ are linearly aligned with separations of 0.1 mm. These electrodes, serving as source, gate, and drain for transport measurements, respectively, are surrounded by a guard electrode in the shape of rectangular frame. A tungsten filament is placed about 1 cm right above the PCB and serves as an electron source. A rectangular shape capacitor is attached to the PCB as a liquid-helium level meter. The entire cell is attached to the mixing chamber of a dilution refrigerator which can reach a base temperature of 15 mK.

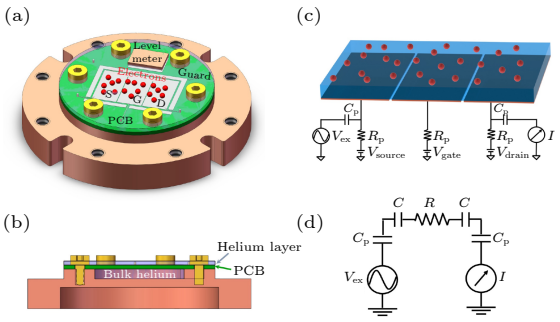

Fig. 1. (a) Schematic drawing of the main components of the experimental setup. The tungsten filament and the mating enclosure are not shown for the purpose of clarity. (b) Side view of the setup. (c) Schematic drawing of transport measurement setup. Bias voltages were applied to the three panel electrodes via protective resistors of $R_\mathrm{p} = 10\,\mathrm{M\Omega}$. The ac voltage source and current meter are capacitively coupled to the source and drain electrodes via capacitors of $C_\mathrm{p} = 1\,\mu\mathrm{F}$. (d) Lumped-circuit model for result analyses.

To prepare a 2DES, the cell was firstly emptied and cooled below 1 K. Here, ^{4}He gas was admitted to the experimental cell through a capillary later. The dosage was calibrated at room temperature in advance, which guarantees a liquid surface above the electrodes by 1 mm. After the helium stabilized (determined by cease of fluctuation for the mixing chamber temperature), positive voltages ($V_0 > 0$) were applied to all the three rectangular panel electrodes, and a negative voltage ($V_\mathrm{guard} < 0$) to the guard electrode. This builds a potential well to restrict electrons within the guard frame. A high current pulse was then applied through the tungsten filament for electron emission (see the Supplemental Materials[19] for details). The emitted electrons flew towards the helium surface, and some of them bound to the helium surface to form the 2DES.

Different from conventional transport measurements for solid-state systems, the 2DES floating above helium surface is isolated from the source and drain electrodes. Consequently, the electrodes are capacitively coupled to the 2DES and the total number of electrons is constant [as shown in Fig. 1(c)]. In this sense, transport measurements must be conducted at relatively high frequency. The voltage excitation was superimposed to the bias voltage on the source electrode and modulated the chemical potential of electrons in this area. The modulation transmits a planar motion of electrons across the entire 2DES, and is detected by the drain electrode in terms of sinusoidal currents. Overall, the transport process can be simplified by a lumped-circuit model in which the 2DES is seen as a resistor as shown in Fig. 1(d). However, the transmission line model[20–22] has been employed for more precise analyses.

All transport measurements presented in this work were conducted at 50 mK. It was firstly conducted on a 2DES prepared with the three panel electrodes biased at $V_0 = +10\,\mathrm{V}$ and the guard at $V_\mathrm{guard} = -2.5\,\mathrm{V}$. The magnitude of excitation voltage is $V_\mathrm{ac} = 0.1\,\mathrm{V}$ and its frequency is 2.107 kHz. We observed non-zero current as the 2DES was firstly prepared, which gradually vanished as the gate voltage V_gate was tuned to negative values. The current was recovered when V_gate was swept towards positive values again, exhibiting a clear and sudden onset for the imaginary component of the current [I_y, see Fig. 2(a)] at $V_\mathrm{gate} = V_\mathrm{on} = 0.3\,\mathrm{V}$. The onset was followed by a decrease, being mild at first but accelerating as V_gate increased. I_y vanished again with a sharp cutoff at around $V_\mathrm{gate} = V_\mathrm{cut} = 30.5\,\mathrm{V}$. Meanwhile, the real component [I_x, see Fig. 2(b)] exhibits a peak at the onset, and remains negligible afterwards.

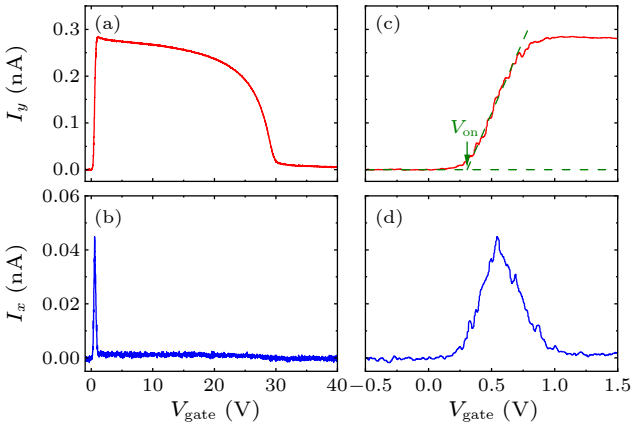

Fig. 2. [(a), (b)] I_y and I_x as functions of V_gate. [(c), (d)] Zoom-in views of (a) and (b) to focus on the onset. The onset voltage V_on is determined by extrapolating the rising slope as demonstrated by the green dashed lines.

Because of the capacitive couplings between electrodes and the 2DES, I_y represents the dynamic response to the voltage excitation while I_x is a measure of dissipation. At the beginning of the sweep, the negative value of V_gate builds a potential barrier in the gate area which expels electrons to the source and drain areas. The increase of V_gate lowers the barrier height and allows electrons to enter the gate area. These electrons build a connection between the source and drain as indicated by the current onset. The

barrier changes to a potential well when $V_{\rm gate}$ surpasses V_0, leading to a higher electron density in the gate area. It eventually depletes the source and drain areas as indicated by the current cutoff. We also performed transport measurements at various frequencies between 2.107 kHz and 49.91 kHz. As shown in Figs. 3(c) and 3(d), the current onset shifts from 0.5 V to 1.3 V as frequency increases. In the meantime, the cutoff shifts to lower $V_{\rm gate}$ at higher frequencies, from 30.5 V to 29.0 V.

We can make use of the onset and cutoff to estimate the average electron density n. Potential difference between neighboring areas is created by the different bias voltages applied to neighboring electrodes. This difference will be compensated by the distribution of electrons to maintain a homogeneous chemical potential. Considering that the frequency-related shifts of $V_{\rm on}$ and $V_{\rm cut}$ are remarkably small compared with their difference from V_0, we can reliably use the values measured at 2.107 kHz for the estimate: the potential difference between gate the and rest areas, $\Delta V_{\rm on} = V_0 - V_{\rm on} = \frac{3ne}{2} \cdot \frac{A}{C}$ gives the average density $n = 3.8 \times 10^7\,{\rm cm}^{-2}$. As $V_{\rm gate}$ is changed, $n_{\rm s} = n_{\rm d} = 3n/2 = 5.7 \times 10^7\,{\rm cm}^{-2}$ when the gate area is depleted before the onset, and $n_{\rm g} = 3n = 1.14 \times 10^8\,{\rm cm}^{-2}$ when the source and drain areas are depleted after the cutoff.

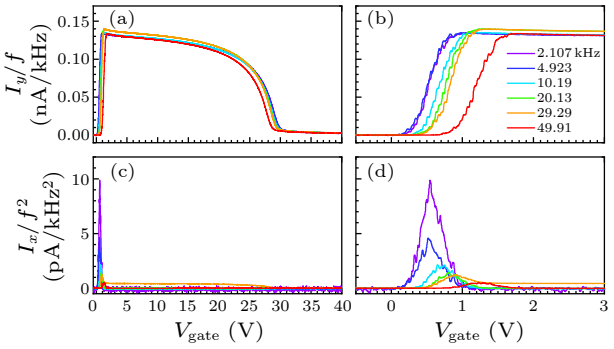

Fig. 3. Experimental results measured at multiple frequencies as labeled in the legends. [(a), (b)] I_y/f and I_x/f^2 as functions of $V_{\rm gate}$. I_y and I_x are normalized to f and f^2 respectively for convenience of comparison. [(c), (d)] Zoom-in views of (a) and (b) at the onset transitions.

Given the sinusoidal excitation applied to the source electrode, the potential of the electrons in the source area is modulated. Such modulation triggers the electron motion between the source and gate areas, which transmits to the drain area via Coulomb interactions. The transmission is capacitively coupled to the panel electrodes and can be analyzed with a transmission-line model. For the specific geometry of our device, the current detected by the drain electrode is complex, given by [21,23]

$$I = I_0(1+j)\Big(\frac{3\delta}{2\,L}\Big)\frac{\sinh^2(jkL)}{\sinh(3jkL)}, \tag{1}$$

where $I_0 = V_{\rm ex}\omega C/3$, $k = (1-j)/\delta$ is the complex wavevector of the current which is associated with the conductivity of the 2DES (σ) and the areal capacitance to the electrodes ($c = C/A$) by $\delta = \sqrt{\frac{2\sigma}{\omega c}}$. Here δ is a measure of penetration length within the 2DEG. Our results are in qualitative consistence with the model in that the onset transition shifts to higher $V_{\rm gate}$ for higher frequency. [19] The boundaries of the gate area adjacent to the source and drain are the bottleneck for the transport process at the onset when the connection is about to be built. The connection is built when the penetration depth δ is larger than the width of the gate electrode W; δ shrinks with an increasing frequency, thus more electrons are needed to maintain the penetration depth, leading to the transition shift to higher $V_{\rm gate}$. The same reason can be applied to the cutoffs, where electrons are depleted from the source and drain by the gate. Notably, δ is smaller for higher frequency, leading to an earlier cutoff compared with that for lower frequencies.

However, our results are not in quantitative agreement with the transmission-line model. Negative I_y is predicted by the model right before the onset of connection, [19] which has been experimentally observed before. [23] Such a behavior, more obvious for higher frequencies, is a signature of phase change when the surpass of δ over W takes place. We did not observe such behavior at any frequency. One possible reason is the existence of Wigner crystal (WC) phase [17,18] for our measurement at 50 mK, while the other study was conducted above 1.3 K. [23] The formation of WC increases the rigidity of the electron system, thus leading to a sharper onset. In addition, the fact that $\delta \propto \sqrt{\sigma/\omega}$ suggests that the electron density in the gate area ($n_{\rm g}$) should scale with the measurement frequency when onset occurs. However, we only observed a five-fold increase of $n_{\rm g}$ while ω increases by about 25 times. This is likely related with the nonlinearity arising from the interaction between the WC and dimple lattice, [24] and more complexity could be introduced by the inhomogeneity in electron motion due to the potential gradient while ripplon excitations of helium surface are not affected.

The total number of electrons and the average areal density are fixed once the 2DES is formed. Therefore, tuning the electron density should be conducted at the preparation stage. We demonstrate effective tuning by controlling the bias voltages V_0 on the panel electrodes during the electron emission. The emission is isotropic in space and broad in kinetic energy. The bias voltage exerts a vertical electric field to accelerate the electrons towards the helium surface. Only the part of electrons within appropriate energy and momentum windows are able to bind to the surface with the rest drained to ground either through the helium layer and the electrodes, or directly through the cell's metallic wall. The bound electrons themselves form a negatively charged layer that screens the vertical field, thus preventing further deposition. In this sense, the charge density is directly associated with the magnitude of the field, and the bias voltage V_0 plays an important tuning knob to control the quantity of trapped electrons.

We prepared six 2DESs with V_0 ranging from 10 to 100 V. As shown in Fig. 4(a), all 2DESs exhibit a window of current detection similar to the one shown in Fig. 2(a).

The increases of $V_{\rm on}$, $V_{\rm cut}$, and the window width all shift to larger values with V_0, evidently convincing that the quantity of bound electrons indeed increases. This is further supported by the monotonic increase of I_y's peak value at onsets. The average density n ranges between $3.8\times10^7\,{\rm cm}^{-2}$ and $3.2\times10^8\,{\rm cm}^{-2}$ and scales with V_0 for $V_0 < 60\,{\rm V}$ with a slope of $3.5\times10^6\,{\rm cm}^{-2}\cdot{\rm V}^{-1}$. This is close to the coefficient for the linearity of saturated density against V_0: $n_{\rm s} = 2\epsilon\epsilon_0 V_0/3ed$,[19] giving a slope of $3.87\times10^6\,{\rm cm}^{-2}\cdot{\rm V}^{-1}$. Here $\epsilon = 1.057$ is the dielectric constant of liquid helium, and ϵ_0 is the permittivity of vacuum. The difference is less than 10% and could be accounted for by the blurring of electric field[19] considering the relative large thickness of the helium layer (1 mm) compared with the gap between electrodes (0.1 mm).

A slight deviation exists for $V_0 > 60\,{\rm V}$ in coincidence with abnormal transport behaviors for the 2DESs prepared with $V_0 = 80\,{\rm V}$ and 100 V, both experience abrupt cutoffs in I_y at $V_{\rm gate} = 152\,{\rm V}$. The abnormality is due to the instability and collapse of helium surface caused by high electron density.[25,26] As a result, n is underestimated because there are still electrons left in the source and drain areas at the collapse. In fact, a majority of electrons accumulate in the gate area when the abrupt cutoff happens, and the local density $n_{\rm g} \approx 3n = (7.5\sim9.0)\times10^8\,{\rm cm}^{-2}$ for these two 2DESs, close to the critical density for the collapse ($2.5\times10^9\,{\rm cm}^{-2}$).[27] The difference again could be due to the blurring of electric field which may lead to inhomogeneity of electron distribution. Additionally, n of the 2DES with $V_0 = 60\,{\rm V}$ is also slightly smaller than the linear dependence, which could be attributed to the non-negligible screening effect of electrons to the electric field.

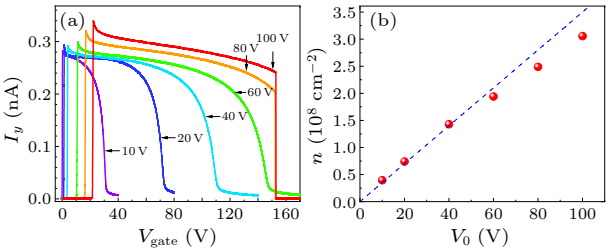

Fig. 4. (a) I_y as a function of $V_{\rm gate}$ for the 2DESs prepared with different V_0. All measurements were performed at 2.107 kHz. Values of V_0 are labeled to each curve. (b) Dependence of n on V_0. The blue dashed line is a linear fit of the lowest three densities.

We have demonstrated the successes in preparation of 2DESs floating on surfaces of liquid helium, conduction of transport measurements to comprehensively characterize its properties, and manipulations of the electron distribution using FET technique. Nonetheless, it is undeniable that our contemporary findings reveal certain limitations. We hereby explore a detailed discussion of strategies for enhancements as follows.

Density is a crucial tuning knob for electron interactions. On the one hand, it is tempting to extend the lower density limit to fabricate single-electron devices. On the other hand, it is also interesting to extend the upper limit to demonstrate quantum mechanical effects of strong correlations. Specifically, the lower limit of carrier density for GaAs/AlGaAs heterostructures is on the order of $10^{10}\,{\rm cm}^{-2}$.[28–30] It would be of great significance for the 2DES on helium surface to reach this level in order to present a full transition series from classical electron gases to strongly correlated quantum systems. In our current setup, the electrons generated by a single emission are more than enough to saturate the surface so that the density is determined solely by V_0. A shorter pulse time will not raise the filament to a threshold temperature for emission, and a smaller V_0 cannot guarantee precise control and reproducibility of electron density. A cold-emission technique has been proposed instead for lower dosages by shedding ultraviolet light on zinc thin films.[31] The dosage could be 3–4 orders of magnitude lower than the hot emission from tungsten filament, and multiple emissions are allowed. Using this technique, low density and fine tuning can be realized. As for the other extreme, the upper limit is ascribed to the instability of helium surface induced by the interplay of gravity, the surface tension, and the pressure of the electrons on the surface.[25,26] Reducing the helium layer thickness within 100 nm can strengthen its hydrodynamic rigidity due to the van der Waals interaction from the substrate and hence relief the instability. In addition, fringing effect inevitably exists and will blur potential profiles defined by the voltages applied to electrodes, causing difficulties for manipulating electrons. An effective way to minimize the fringing effect is to prepare a thin helium layer.[19] Reducing the thickness of the helium layer will also sharpen the potential well, enabling better manipulations. However, bringing 2DESs close to the electrodes will also introduce microscopic fluctuation to the potential profile due to the roughness of the electrodes. This will reduce electrons' mobility. Amorphous electrodes have been proposed to release such drawbacks.

In summary, we have successfully prepared two-dimensional electron systems floating on superfluid helium surfaces. The electron density can be controlled over one order of magnitude, from $3.8\times10^7\,{\rm cm}^{-2}$ to $3.2\times10^8\,{\rm cm}^{-2}$. By modulating bias voltage on the source electrode, we are able to conduct transport measurements to characterize the 2DESs. We realize manipulation of electron distribution using FET technique and tuning of electron motions by variating frequency. Our work has made a solid foundation to extend scientific research on low-dimensional electron systems and many-body physics based on 2DESs on helium surface. Further work is needed to enhance the advantages in high tunability of electron density, high mobility, and feasible controllability.

Acknowledgments. This work was supported by the Beijing Natural Science Foundation (Grant No. JQ21002), the National Natural Science Foundation of China (Grant No. T2325026), the National Key R&D Program of China (Grant No. 2021YFA1401902), the Key Research Program of Frontier Sciences, CAS (Grant No. ZDBS-LY-SLH0010), and the CAS Project for Young Scientists in Basic Research (Grant No. YSBR-047).

References

[1] Klitzing K V, Dorda G, and Pepper M 1980 *Phys. Rev. Lett.* **45** 494
[2] Tsui D C, Stormer H L, and Gossard A C 1982 *Phys. Rev. Lett.* **48** 1559
[3] Reyren N, Thiel S, Caviglia A D, Kourkoutis L F, Hammerl G, Richter C, Schneider C W, Kopp T, Ruetschi A S, Jaccard D, Gabay M, Muller D A, Triscone J M, and Mannhart J 2007 *Science* **317** 1196
[4] Gariglio S, Reyren N, Caviglia A D, and Triscone J M 2009 *J. Phys.: Condens. Matter* **21** 164213
[5] Liu C J, Yan X, Jin D F, Ma Y, Hsiao H W, Lin Y L, Bretz-Sullivan T M, Zhou X, Pearson J, Fisher B, Jiang J S, Han W, Zuo J M, Wen J, Fong D D, Sun J, Zhou H, and Bhattacharya A 2021 *Science* **371** 716
[6] Chen Z, Liu Y, Zhang H, Liu Z, Tian H, Sun Y, Zhang M, Zhou Y, Sun J, and Xie Y 2021 *Science* **372** 721
[7] Novoselov K S, Geim A K, Morozov S V, Jiang D, Zhang Y, Dubonos S V, Grigorieva I V, and Firsov A A 2004 *Science* **306** 666
[8] Zhang Y B, Tan Y W, Stormer H L, and Kim P 2005 *Nature* **438** 201
[9] Radisavljevic B, Radenovic A, Brivio J, Giacometti V, and Kis A 2011 *Nat. Nanotechnol.* **6** 147
[10] Splendiani A, Sun L, Zhang Y, Li T, Kim J, Chim C Y, Galli G, and Wang F 2010 *Nano Lett.* **10** 1271
[11] Mak K F, Lee C, Hone J, Shan J, and Heinz T F 2010 *Phys. Rev. Lett.* **105** 136805
[12] Andrei E Y, Lévy F, and Mooser E, eds. 1997 *Two-Dimensional Electron Systems: on Helium and other Cryogenic Substrates* (Netherlands: Springer)
[13] Grimes C C 1978 *Surf. Sci.* **73** 379
[14] Williams F I B 1982 *Surf. Sci.* **113** 371
[15] Sommer W T 1964 *Phys. Rev. Lett.* **12** 271
[16] Monarkha Y and Kono K 2004 *Two-Dimensional Coulomb Liquids and Solids* (Berlin: Springer)
[17] Shirahama K and Kono K 1995 *Phys. Rev. Lett.* **74** 781
[18] Grimes C C and Adams G 1979 *Phys. Rev. Lett.* **42** 795
[19] Supplemental Materials include the details of electron emissions, calculations of saturated electron density, simulations of electron distributions, analyses on transmission-line model, and simulations of potential profile and fringing effect.
[20] Sommer W T and Tanner D J 1971 *Phys. Rev. Lett.* **27** 1345
[21] Mehrotra R and Dahm A J 1987 *J. Low Temp. Phys.* **67** 115
[22] Lea M J, Stone A O, Fozooni P, and Frost J 1991 *J. Low Temp. Phys.* **85** 67
[23] Nasyedkin K, Byeon H, Zhang L, Beysengulov N R, Milem J, Hemmerle S, Loloee R, and Pollanen J 2018 *J. Phys.: Condens. Matter* **30** 465501
[24] Ikegami H, Akimoto H, and Kono K 2009 *Phys. Rev. Lett.* **102** 046807
[25] Gor'kov L P and Chernikova D M 1973 *JETP Lett.* **18** 68
[26] Mima K and Ikezi H 1978 *Phys. Rev. B* **17** 3567
[27] Williams R and Crandall R S 1971 *Phys. Lett. A* **36** 35
[28] Lin X, Du R, and Xie X 2014 *Natl. Sci. Rev.* **1** 564
[29] Nuebler J, Umansky V, Morf R, Heiblum M, Von Klitzing K, and Smet J 2010 *Phys. Rev. B* **81** 035316
[30] Pan W, Masuhara N, Sullivan N S, Baldwin K W, West K W, Pfeiffer L N, and Tsui D C 2011 *Phys. Rev. Lett.* **106** 206806
[31] Shankar S, Sabouret G, and Lyon S A 2010 *J. Low. Temp. Phys.* **161** 410